

**SYNTHESIS AND CHARACTERIZATION OF
POTENTIAL HUMAN HYPOXIA INDUCIBLE
FACTOR (HIF) PROLYL HYDROXYLASE
DOMAIN 2 (PHD-2) INHIBITORS**

TOH LEE ROY

UNIVERSITI SAINS MALAYSIA

2021

**SYNTHESIS AND CHARACTERIZATION OF
POTENTIAL HUMAN HYPOXIA INDUCIBLE
FACTOR (HIF) PROLYL HYDROXYLASE
DOMAIN 2 (PHD-2) INHIBITORS**

by

TOH LEE ROY

**Thesis submitted in fulfilment of the requirements
for the degree of
Master of Science**

April 2021

ACKNOWLEDGEMENT

First, I would like to express my sincere gratitude and appreciation to my supervisor, Dr. Yeoh Kar Kheng for his persistent guidance, inspiration and support that made this study a success. I have received a lot of supports and valuable advices during this study.

I would like to acknowledge Universiti Sains Malaysia for offering me the facilities throughout my study. My sincere thanks also go to all the technical staffs of the School of Chemical Sciences, USM especially Mr. Nizam, Mrs. Wan Zulilawati, Mrs. Asma, Mr. Nazeef, Mr. Ramlee and Miss Alia, who helped during many stages of this study.

I wish to thank my friends and colleagues, Ms. Chong Mui Phin, Mr. Maadh, Mr. Suhaib, Dr. Zuhair and Wong Kok Tong who had encouraged and provided many valuable comments and suggestions during my study.

Finally, my sincere appreciation to my dearest family members who have been very supportive and encouraging throughout my study. They have supported me in every way possible during ups and downs in my life. My parents especially have been selfless in giving me the best of everything. Words cannot express my sincere gratefulness for their constant encouragement and love.

TABLES OF CONTENTS

ACKNOWLEDGEMENT	ii
TABLES OF CONTENTS	iii
LIST OF TABLES	vii
LIST OF FIGURES	viii
LIST OF SCHEMES	xiii
LIST OF ABBREVIATIONS AND SYMBOLS	xiv
LIST OF APPENDICES	xviii
ABSTRAK	xix
ABSTRACT	xx
CHAPTER 1	INTRODUCTION
1.1 Hypoxia inducible factors (HIFs) and HIF hydroxylases	1
1.2 HIF signaling pathways	5
1.3 Problem statement	6
1.4 Research objectives	7
1.5 Scope of study	7
CHAPTER 2	LITERATURE REVIEW
2.1 HIF target genes	9
2.2 Therapeutics benefits of HIF activation	11
2.3 PHD-2 structural data	11
2.4 Computer aided drug design (CADD)	14
2.4.1 Docking and root mean squared deviation (RMSD)	15
2.5 PHD inhibitors	16
2.5.1 Iron chelators	16

2.5.2	Transition metal ions	17
2.5.3	2-Oxoglutarate (2OG) mimetic inhibitors	17
2.5.3(a)	N-oxalylglycine (NOG) and dimethyl N-oxalyl-glycine (DMOG)	18
2.5.3(b)	Thiazol and pyrazole analogues	20
2.5.3(c)	Pyridine analogues, pyridinol analogues and pyrimidine.....	22
2.5.3(d)	Benzodiazole analogues	25
2.5.3(e)	Bicyclic isoquinoline analogues (BIQ)	27
2.5.4	Key interactions of 2-oxoglutarate (2OG) mimetic inhibitors	30

CHAPTER 3 MATERIALS AND METHODS

3.1	Chemicals and solvents	32
3.2	Characterization of the compounds	32
3.2.1	Nuclear magnetic resonance (NMR)	32
3.2.2	Fourier transform infrared spectroscopy (FT-IR)	33
3.2.3	High resolution mass spectrometry (HRMS)	33
3.2.4	Melting point determination	33
3.2.5	Flow of Experiments	34
3.3	Computer aided drug design (CADD)	35
3.3.1	Ligands preparation	35
3.3.2	Ligands generation for docking	35
3.3.3	Protein preparation	35
3.3.4	Grid generation	36
3.3.5	Molecular docking studies	36
3.3.5(a)	Positive control docking	36
3.3.5(b)	Ligands-protein docking	37
3.3.5(c)	Ligands-protein visualization	37

3.4	Chemical Synthesis	37
3.4.1	Synthesis of 2-oxo-2H-chromene-3-carboxylic acid analogues (A1 – A3)	37
3.4.2	Synthesis of triazine and pyrimidine (B and C)	40
3.4.3	Synthesis of benzenesulfonamide analogues (D1 – D4)	42
3.4.4	Synthesis of benzoxazolamine analogues (E1 – E3)	45
3.5	RapidFire PHD-2 hydroxylation assay	48
3.6	Cell lines and culture conditions	49
3.6.1	Compounds treatment and immunoblotting	50

CHAPTER 4 RESULTS AND DISCUSSION

4.1	Inhibitor design	51
4.2	Molecular docking studies	53
4.2.1	Positive control docking	53
4.2.2	Docked conformation	57
4.2.3	Binding affinity	62
4.3	Chemical synthesis	64
4.3.1	2-oxo-2H-chromene-3-carboxylic acid analogues (A1 – A3)	64
4.3.2	Triazine B1	69
4.3.3	Pyrimidine C1	72
4.3.4	Benzenesulfonamide analogues (D1 – D4)	75
4.3.5	Benzoxazolamine analogues (E1 – E3)	76
4.4	Characterization of compounds	78
4.4.1	2-Oxo-2H-chromene-3-carboxylic acid analogues (A1 – A3)	79
4.4.2	Triazine B1	90
4.4.3	Pyrimidine C1	100
4.4.4	Benzenesulfonamide analogues (D1 – D4)	110
4.4.5	Benzoxazolamine analogues (E1 – E3)	121

4.5	<i>In vitro</i> PHD-2 inhibitory studies of potential inhibitors	132
4.5.1	<i>In vitro</i> PHD-2 inhibitory studies of compounds A1 - D4	132
4.5.2	<i>In vitro</i> PHD-2 inhibitory studies of compound E1	135
4.6	Cell-based studies	137
CHAPTER 5 CONCLUSION		
5.1	Conclusion	141
5.2	Future studies	141
REFERENCES		143
APPENDICES		
LIST OF PUBLICATIONS		

LIST OF TABLES

	Page
Table 2.1	Reported IC ₅₀ values of the transition metal ions against PHD-2 17
Table 2.2	Reported IC ₅₀ values of thiazol analogues (8 – 10) and pyrazole analogues (11 – 16) against PHD-2 21
Table 2.3	Reported IC ₅₀ values of pyridine analogues (17 – 18), pyridinol analogues (19 - 22) and pyrimidine (23) against PHD-2 23
Table 4.1	Data of compounds A1 – E1 based on the Lipinski's Rule of 5 optimized by Ghose 53
Table 4.2	The bond distance of the coordination bond and salt bridge formation of compounds A1-E1 compared with positive control, BIQ obtained from docking study..... 57
Table 4.3	The binding affinity of the synthesized compounds (A1 - D4) estimated by Glide 2.5..... 63
Table 4.4	The melting point determination, HRMS and FT-IR of 2-oxo-2H-chromene-3-carboxylic acid analogues (A1 – A3), triazine compound (B), pyrimidine compound (C), benzenesulfonamide analogues (D1 – D4) and benxozamine analogues (E1 – E3)..... 78
Table 4.5	¹ H NMR (500 MHz, δ _H) and ¹³ C NMR (125MHz, δ _C) data of 2-oxo-2H-chromene-3-carboxylic acid analogues (A1 – A3)..... 81
Table 4.6	¹ H NMR (500 MHz, δ _H) and ¹³ C NMR (125MHz, δ _C) data of benzenesulfonamide analogues (D1 – D4)..... 112
Table 4.7	¹ H NMR (500 MHz, δ _H) and ¹³ C NMR (125MHz, δ _C) data of benxozamine analogues (E1 – E3)..... 123
Table 4.8	The half-maximal inhibitory concentration (IC ₅₀) of the reported compounds as PHD-2 inhibitor. ND, not determined..... 133
Table 4.9	The half-maximal inhibitory concentration (IC ₅₀) of the synthesized compounds (E1, E2 and E3) as PHD-2 inhibitor. ND, not determined..... 136

LIST OF FIGURES

	Page
Figure 1.1	Anatomy of HIF-1 α subunit. Basic helix-loop-helix (bHLH), PER-ARNT-SIM (PAS), N-terminal oxygen-dependent degradation domain (NODD), C-terminal oxygen-dependent degradation domain (CODD), C-terminal transactivation domain (C-TAD) and number of amino acid residues (aa) are shown 2
Figure 1.2	HIF signaling pathway during normoxia and hypoxia 6
Figure 2.1	The reported transcriptional targets that are regulated by HIF. Adapted from Chowdhury, et al., 2008 10
Figure 2.2	Binding interaction of BIQ, 1 with PHD-2 enzyme shown in crystal structure with PDB ID: 2hbt. Data is obtained from Research Collaboratory for Structural Bioinformatics Protein Data Bank (RCSB PDB) 12
Figure 2.3	PHD-2 binding pocket with presence of Trp389, Trp258, Met299 and Ilu256 residues. Data is obtained from Research Collaboratory for Structural Bioinformatics Protein Data Bank (RCSB PDB) 13
Figure 2.4	Iron chelators: 2, 3 and 4 17
Figure 2.5	The crystal structure of PHD-2 active site with 5. 5 is shown in yellow while iron (II) is shown in brown. Data is obtained from RCSB PDB 18
Figure 2.6	The crystal structure of PHD-2 active site with 6. 6 was shown in yellow while manganese (II) was shown in purple was used instead of iron (II). Data is obtained from RCSB PDB 19
Figure 2.7	6 and 7 with reported IC ₅₀ values of 6 (6.2 ¹⁰⁵ μ M) against PHD-2 19
Figure 2.8	Thiazol analogues (8 – 10) and pyrazole analogues (11 – 16) 21
Figure 2.9	The crystal structure of PHD-2 active site with 1-(5-chloro-6-fluoro-1H-benzimidazol-2-yl)-1H-pyrazole-4-carboxylic acid, 16. 16 was shown in yellow while iron (II) was shown in brown Data is obtained from RCSB PDB 22
Figure 2.10	Pyridine analogues (17 - 18), pyridinol analogues (19 - 22) and pyrimidine (23)..... 23

Figure 2.11	The crystal structure of PHD-2 active site with Vadadustat, 22 . 22 was shown in yellow while manganese (II) (substituting iron (II)) was shown in purple. Data is obtained from RCSB PDB	24
Figure 2.12	The crystal structure of PHD-2 active site with (6-hydroxy-1,3-dimethyl-2,4-dioxo-1,2,3,4-tetrahydropyrimidine-5-carbonyl)glycine, 23 . 23 was shown in yellow while Mn(II) (substituting Fe(II)) was shown in purple. Data is obtained from RCSB PDB	25
Figure 2.13	Benzodiazole analogues (24 – 26) with IC ₅₀ values of 24 (100 μM), 25 (0.73 μM) and 26 (12.6 μM) against PHD-2	26
Figure 2.14	The crystal structure of PHD-2 active site with N-[(5,6-dichloro-1H-benzimidazol-2-yl)carbonyl]glycine, 26 . 26 was shown in yellow while iron (II) was shown in brown. Data is obtained from RCSB PDB	26
Figure 2.15	BIQ analogues (27 – 30) with IC ₅₀ values of 27 (0.07 μM), 28 (0.512 μM), 29 (230 μM) and 30 (1.4 μM) against PHD-2	27
Figure 2.16	The crystal structure of PHD-2 active site with N-[(1-chloro-4-hydroxyisoquinolin-3-yl)carbonyl]glycine, 27 . 27 was shown in yellow while iron (II) was shown in brown. Data is obtained from RCSB PDB	28
Figure 2.17	The crystal structure of PHD-2 active site with (2S)-2-([(1-chloro-4-hydroxyisoquinolin-3-yl)carbonyl]amino)propanoic acid, 29 . 29 was shown in yellow while iron (II) was shown in brown. Data is obtained from RCSB PDB	29
Figure 2.18	The crystal structure of PHD-2 active site with N-[(4-hydroxy-8-iodoisoquinolin-3-yl)carbonyl]glycine, 30 . 30 was shown in yellow while iron (II) was shown in brown. Data is obtained from RCSB PDB	30
Figure 3.1	Flow of experiment	34
Figure 4.1	Structures of the potential PHD-2 inhibitors. 2-oxo-2H-chromene-3-carboxylic acid analogues (A1 - A3), triazine compound (B), pyrimidine compound (C), benzenesulfonamide analogues (D1 - D4) and benzoxazolamine analogues (E1 – E3).	21

Figure 4.2	(A) Superimposition of redocked BIQ (yellow) and cocrystalline BIQ (green) in PHD-2 enzyme. (B) The docked conformation of compound BIQ in PHD-2 enzyme. Iron (II) ion is shown in brown colour while the BIQ compound is shown in yellow colour.....	56
Figure 4.3	Docked structure of A1 with PHD2 enzyme. Iron (II) ion is shown in brown colour while the A1 compound is shown in blue colour.....	58
Figure 4.4	Docked structure of B with PHD2 enzyme. Iron (II) ion is shown in brown colour while the B compound is shown in blue colour.....	59
Figure 4.5	Docked structure of C with PHD2 enzyme. Iron (II) ion is shown in brown colour while the C compound is shown in blue colour.....	60
Figure 4.6	Docked structure of D1 compound with PHD2.Fe(II) complex. Iron (II) ion is shown in brown colour while the D1 compound is shown in blue colour.....	61
Figure 4.7	Docked structure of E1 compound with PHD2.Fe(II) complex. Iron (II) ion is shown in brown colour while the E1 compound is shown in blue colour.....	62
Figure 4.8	The proposed mechanism of nucleophilic addition reaction of a diethyl malonate to benzaldehyde to form compound A1	66
Figure 4.9	The proposed mechanism of nucleophilic addition reaction of a benzaldehyde to Meldrum's acid to form compound A2	67
Figure 4.10	The proposed mechanism of nucleophilic addition reaction of an acrylonitrile to benzaldehyde to form compound A3	69
Figure 4.11	The proposed mechanism of nucleophilic addition reaction to form compound B	71
Figure 4.12	The proposed mechanism of nucleophilic addition reaction to form compound C	74
Figure 4.13	The proposed mechanism of nucleophilic addition reaction to form benzenesulfonamide analogues (D1 – D4).....	76
Figure 4.14	The proposed mechanism of nucleophilic addition reaction to form benzoxzolaamine analogues (E1 – E3).....	77
Figure 4.15	¹ H NMR Spectrum of A1	82
Figure 4.16	¹³ C NMR Spectrum of A1	83

Figure 4.17	$^1\text{H} - ^1\text{H}$ COSY Spectrum of A1	84
Figure 4.18	HSQC Spectrum of A1	85
Figure 4.19	HMBC Spectrum of A1	86
Figure 4.20	Selected HMBC correlation of A1	87
Figure 4.21	IR Spectrum of A1	88
Figure 4.22	Mass Spectrum of A1	89
Figure 4.23	^1H NMR Spectrum of B	92
Figure 4.24	^{13}C NMR Spectrum of B	93
Figure 4.25	$^1\text{H} - ^1\text{H}$ COSY Spectrum of B	94
Figure 4.26	HSQC Spectrum of B	95
Figure 4.27	HMBC Spectrum of B	96
Figure 4.28	Selected HMBC correlation of B	97
Figure 4.29	IR Spectrum of B	98
Figure 4.30	Mass Spectrum of B	99
Figure 4.31	^1H NMR Spectrum of C	102
Figure 4.32	^{13}C NMR Spectrum of C	103
Figure 4.33	$^1\text{H} - ^1\text{H}$ COSY Spectrum of C	104
Figure 4.34	HSQC Spectrum of C	105
Figure 4.35	HMBC Spectrum of C	106
Figure 4.36	Selected HMBC correlation of C	107
Figure 4.37	IR Spectrum of C	108
Figure 4.38	Mass spectrum of C	109
Figure 4.39	^1H NMR Spectrum of D1	113
Figure 4.40	^{13}C NMR Spectrum of D1	114
Figure 4.41	$^1\text{H} - ^1\text{H}$ COSY Spectrum of D1	115
Figure 4.42	HSQC Spectrum of D1	116
Figure 4.43	HMBC Spectrum of D1	117

Figure 4.44	Selected COSY and HMBC correlation of D1	118
Figure 4.45	IR Spectrum of D1	119
Figure 4.46	Mass spectrum of D1	120
Figure 4.47	¹ H NMR Spectrum of E1	124
Figure 4.48	¹³ C NMR Spectrum of E1	125
Figure 4.49	¹ H – ¹ H COSY Spectrum of E1	126
Figure 4.50	HSQC Spectrum of E1	127
Figure 4.51	HMBC Spectrum of E1	128
Figure 4.52	Selected COSY and HMBC correlation of E1	129
Figure 4.53	IR Spectrum of E1	130
Figure 4.54	Mass Spectrum of E1	131
Figure 4.55	Structure of Roxadustat, FG-4592.....	132
Figure 4.56	Benzoxazolamine analogues E1 , F2a and F2b	135
Figure 4.57	Log concentration versus % PHD-2 inhibition curve for FG-4592 , E1 , F2a and F2b	137
Figure 4.58	Effects of F2a and F2b acids and E2 and E3 esters on cellular HIF-1 α levels: (A, B) Immunoblots showing no HIF-1 α stabilization in the presence of F2a and F2b (200 μ M and 1 mM) in MDA-MB-231 and MCF-7 cells after 6 hours incubation. (C, D) Immunoblots showing no induction of HIF-1 α in A549 cells after treated with the indicated concentrations of F2a , F2b , E2 and E3 in 1% of DMSO (C) and 2% of DMSO (D) for 6 h. DMSO (1% or 2%) were used as a negative control; FG-4592 was used as a positive control. β -actin and Ponceau S stain were used as a loading control.....	140

LIST OF SCHEMES

	Page
Scheme 1.1 The hydroxylation reactions catalyzed by HIF prolyl hydroxylase domains (PHDs) and Factor inhibiting HIF (FIH)	3
Scheme 1.2 The proposed mechanism of action of 2OG dependent oxygenases	4
Scheme 4.1 Synthetic procedures for the preparation of 2-oxo-2H-chromene-3-carboxylic acid analogues (A1 - A3). Method A - C	64
Scheme 4.2 Synthetic procedures for the preparation of compound B	70
Scheme 4.3 Synthetic procedures for the preparation of compound C	72
Scheme 4.4 Synthetic procedures for the preparation of benzenesulfonamide analogues (D1 - D4).....	75
Scheme 4.5 Synthetic procedures for the preparation of benzoxazamine analogues (E1 - E3).....	77

LIST OF ABBREVIATIONS AND SYMBOLS

1D	1 dimension
2D	2 dimensions
2OG	2-oxoglutarate
α -KG	α -ketoglutarate
Aa	Amino acid
ACD	Anemia of chronic disease
Acetone-d ₆	Deuterated acetone
Ala	Alanine
Arg383	Arginine residue 383
Asn803	Asparagine residue 803
Asp201	Aspartic acid residue 201
Asp315	Aspartic acid residue 315
bHLH	Basic helix-loop-helix
BIQ	Bicyclic isoquinoline
CADD	Computer aided drug design
CKD	Chronic kidney disease
CODD	C-terminal oxygen-dependent degradation domain
COSY	Correlated spectroscopy
C-TAD	C-terminal transactivation domain
δ	Chemical shift value
<i>d</i>	doublet
DABCO	1,4-Diazabicyclo[2.2.2]octane
°C	Degree Celsius
DCM	Dichloromethane
DFO	Desferrioxamine

DIPEA	Diisopropylethylamine
DMOG	Dimethyl N-oxalyl-glycine
DMSO	Dimethylsulfoxide
DMSO-d6	Deuterated dimethylsulfoxide
DNA	Deoxyribonucleic acid
EPO	Erythropoietin
ESI	Electrospray ionization
EtOAc	Ethyl acetate
FAS	Ferrous ammonium sulphate
FIH	Factor inhibiting HIF
FT-IR	Fourier transform infrared spectroscopic
g	gram
HIF	Hypoxia inducible factor
His199	Histidine residue 199
His279	Histidine residue 279
His313	Histidine residue 313
His374	Histidine residue 374
HMBC	Heteronuclear multiple bond correlation
HRMS	High resolution mass spectrometry
HRP	Horseradish peroxidase
HSQC	Heteronuclear single quantum correlation
IC ₅₀	Half-maximal inhibitory concentration
ID	Identification document
IgG	Immunoglobulin G
Ile256	Isoleucine residue 256
<i>J</i>	Coupling constant
JmjC	Jumonji

KBR	Potassium bromide
L-AA	L-Ascorbic acid
LLC	Limited liability company
m.p.	Melting point
m/z	Mass to charge ratio
MeOH	Methanol
Met299	Methionine residue 299
mg	milligram
ml	Milliliter
mmol	millimole
Mol	mole
MS	Mass spectrometry
N	Normality
NMR	Nuclear magnetic resonance
NODD	N-terminal oxygen-dependent degradation domain
NOG	N-oxalylglycine
ODD	Oxygen-dependent degradation domain
<i>p</i>	Pentet
PAGE	Polyacrylamide gel electrophoresis
PAS	Per-ARNT-Sim
PBS	Phosphate-buffered saline
PDB	Protein data bank
pH	Potential of hydrogen
PHD	Prolyl hydroxylase domain
ppm	Part per million
Pro402	Proline residue 402
Pro564	Proline residue 564

PVDF	Polyvinylidene difluoride
pVHL	Von Hippel-Lindau tumor suppressor protein
<i>q</i>	quartet
QTOF	Quadrupole-time-of-flight
RBC	Red blood cells
RCSB	Research collaboratory for structural bioinformatics
R_f	Retention factor
RF-MS	RapidFire mass
RMSD	Root mean square deviation
<i>s</i>	singlet
SDS	Sodium dodecyl sulfate
SP	Standard precision
SPE	Solid phase extraction
<i>t</i>	triplet
TLC	Thin layer chromatography
Trp258	Tryptophan residue 258
Trp389	Tryptophan residue 389
μL	Microlitre
UPLC	Ultra-performance liquid chromatography
VEGF	Vascular endothelial growth factor

LIST OF APPENDICES

- APPENDIX A DOCKED STRUCTURE OF **A2** COMPOUND WITH PHD2.FE(II) COMPLEX. **A2** COMPOUND CHELATED THE Fe^{2+} ION (BROWN) VIA THE OXYGEN ATOMS IN A BIDENTATE MANNER AND FORMED SALT BRIDGE WITH ARG383 RESIDUE VIA CARBOXYLATE OXYGEN ATOM.
- APPENDIX B DOCKED STRUCTURE OF **A3** COMPOUND WITH PHD2.FE(II) COMPLEX. **A3** COMPOUND CHELATED THE Fe^{2+} ION (BROWN) VIA THE OXYGEN ATOMS IN A BIDENTATE MANNER AND FORMED SALT BRIDGE WITH ARG383 RESIDUE VIA CARBOXYLATE OXYGEN ATOM.
- APPENDIX C DOCKED STRUCTURE OF **D2** COMPOUND WITH PHD2.FE(II) COMPLEX. **D2** COMPOUND CHELATED THE Fe^{2+} ION (BROWN) VIA THE OXYGEN ATOMS IN A BIDENTATE MANNER AND FORMED SALT BRIDGE WITH ARG383 RESIDUE VIA CARBOXYLATE OXYGEN ATOM.
- APPENDIX D DOCKED STRUCTURE OF **D3** COMPOUND WITH PHD2.FE(II) COMPLEX. **D3** COMPOUND CHELATED THE Fe^{2+} ION (BROWN) VIA THE OXYGEN ATOMS IN A BIDENTATE MANNER AND FORMED SALT BRIDGE WITH ARG383 RESIDUE VIA CARBOXYLATE OXYGEN ATOM.
- APPENDIX E DOCKED STRUCTURE OF **D4** COMPOUND WITH PHD2.FE(II) COMPLEX. **D4** COMPOUND CHELATED THE Fe^{2+} ION (BROWN) VIA THE OXYGEN ATOMS IN A BIDENTATE MANNER AND FORMED SALT BRIDGE WITH ARG383 RESIDUE VIA CARBOXYLATE OXYGEN ATOM.

**SINTESIS AND PENCIRIAN PERENCAT FAKTOR PENDORONG
HIPOKSIA MANUSIA (HIF) PROLIL HIDROKSILASI 2 (PHD-2) YANG
BERPOTENSI**

ABSTRAK

Perencatan farmakologi enzim prolil hidroksilase domain (PHD) telah disarankan sebagai kaedah alternatif untuk menaikan peraturan faktor induktif hipoksia (HIF) dan berfungsi sebagai kaedah terapi untuk penyakit seperti anemia dan penyakit kardiovaskular. Kajian ini bertujuan untuk menilai lima siri sebatian: asid 2H-chromene-3-karbosilik (**A1 - A3**), triazin (**B**), pirimidin (**C**), benzenesulfonamid (**D1 - D4**), dan benzoxazolamine (**E1 - E3**) sebagai inhibitor perencat PHD-2. Mod pengikatan dan tenaga bebas **A1 - E3** pertama kali dinilai menggunakan kajian sambungan molekul. Hasil dok menunjukkan bahawa semua sebatian yang diuji mampu mengikat ke tapak aktif PHD-2 secara bidentate dan membentuk interaksi jambatan garam dengan residu asid amino Arg383 selain daripada menunjukkan tenaga bebas pengikatan yang istimewa. Sebatian kemudian disintesis dan dicirikan menggunakan FT-IR, HRMS, NMR ¹H, ¹³C NMR dan 2D NMR untuk mengesahkan struktur. **A1 - E3** kemudian disaring untuk potensi penghambatan mereka terhadap PHD-2 menggunakan PHD-2 RapidFire assay. Hasil penghambatan menunjukkan bahawa sebatian **E1** adalah perencat PHD-2 yang kuat, dengan nilai IC₅₀ 17,45 μM. Sebaliknya, etil ester **E2** dan **E3** disintesis dan diuji dalam kajian berasaskan sel. Namun, mereka tidak menunjukkan kemampuan untuk menginduksi HIF-1α sebagai petunjuk perencat PHD-2 selular.

**SYNTHESIS AND CHARACTERIZATION OF POTENTIAL HUMAN
HYPOXIA INDUCIBLE FACTOR (HIF) PROLYL HYDROXYLASE
DOMAIN 2 (PHD-2) INHIBITORS**

ABSTRACT

Pharmacological inhibition of prolyl hydroxylase domain (PHD) enzymes have been suggested as an alternative method to upregulate hypoxia inducible factor (HIF) and serve as a therapeutic method for diseases such as anemia and cardiovascular disease. This study aims at evaluating five series of compounds: 2H-chromene-3-carboxylic acids (**A1 – A3**), triazine (**B**), pyrimidine (**C**), benzenesulfonamides (**D1 – D4**), and benzoxazolamine (**E1 – E3**) as PHD-2 inhibitors. The binding modes and free energies of **A1 – E3** were first evaluated using molecular docking studies. The docking results demonstrated that all the tested compounds were capable of binding to the PHD-2 active site in a bidentate manner and forming salt bridge interaction with amino acid residue Arg383 apart from displaying preferential free energies of binding. The compounds were subsequently synthesized and characterized using FT-IR, HRMS, ¹H NMR, ¹³C NMR and 2D NMR to confirm the structures. **A1 – E3** were then screened for their inhibitory potencies against PHD-2 using a PHD-2 RapidFire assay. The inhibitory results revealed that compound **E1** was a potent PHD-2 inhibitor, with IC₅₀ value of 17.45 μM. On the other hand, ethyl ester **E2** and **E3** were synthesized and tested in cell-based study. However, they showed no ability to induce HIF-1α as an indicator of cellular PHD-2 inhibition.

CHAPTER ONE

INTRODUCTION

1.1 Hypoxia inducible factors (HIFs) and HIF hydroxylases

Hypoxia is a condition whereby there is a lack of oxygen in body tissues with reduced oxygen levels as low as or less than 2% of oxygen concentration¹. Hypoxia inducible factors (HIFs) are heterodimeric transcription factors composed of α and β subunits^{2,3}. There are three α subunits [HIF-1 α , HIF-2 α and HIF-3 α] and three β subunits (HIF-1 β , HIF-2 β and HIF-3 β)^{4,5}.

HIF-1 α is the most extensively studied and was first identified by Semenza, Wang and co-workers^{2,6-10}. HIF-1 α possess a full central oxygen-dependent degradation domain (ODD) which is absent in HIF- β ^{11,12}. There are two transactivation domains exist within ODD of HIF-1 α , N-terminal named NODD containing Pro402 and C-terminal named CODD containing Pro564¹³⁻¹⁵, which enable the degradation of HIF-1 α . HIF-1 α is also hydroxylated at an asparagine residue (Asn803 in HIF-1 α) at C-terminal transactivation domain (C-TAD)¹².

HIF-1 α is ubiquitously expressed^{1,11,16,17}. Expression of HIF-1 α is induced by hypoxia, tissue ischemia or regulated by cellular oxygen tension and hence HIF-1 α is a regulatory protein^{2,8,18-22}. HIF-1 β is a constitutive nuclear protein which constitutively expressed regardless of changes in oxygen availability²³. Anatomy of HIF-1 α is shown in **Figure 1.1**.

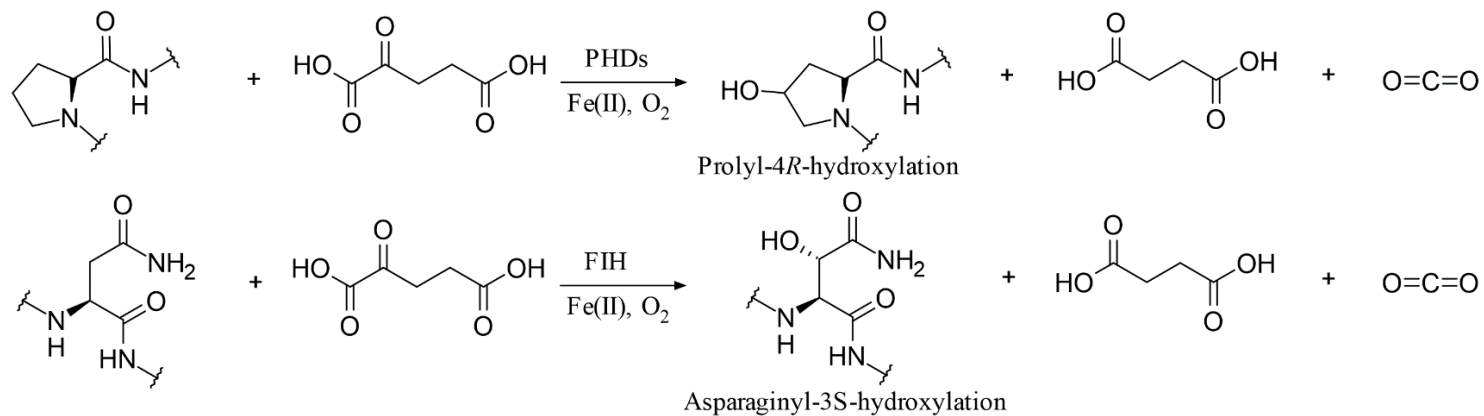


Figure 1.1: Anatomy of HIF-1 α subunit. Basic helix-loop-helix (bHLH), Per-ARNT-Sim (PAS), N-terminal oxygen-dependent degradation domain (NODD), C-terminal oxygen-dependent degradation domain (CODD), C-terminal transactivation domain (C-TAD) and number of amino acid (aa) residues are shown²⁴.

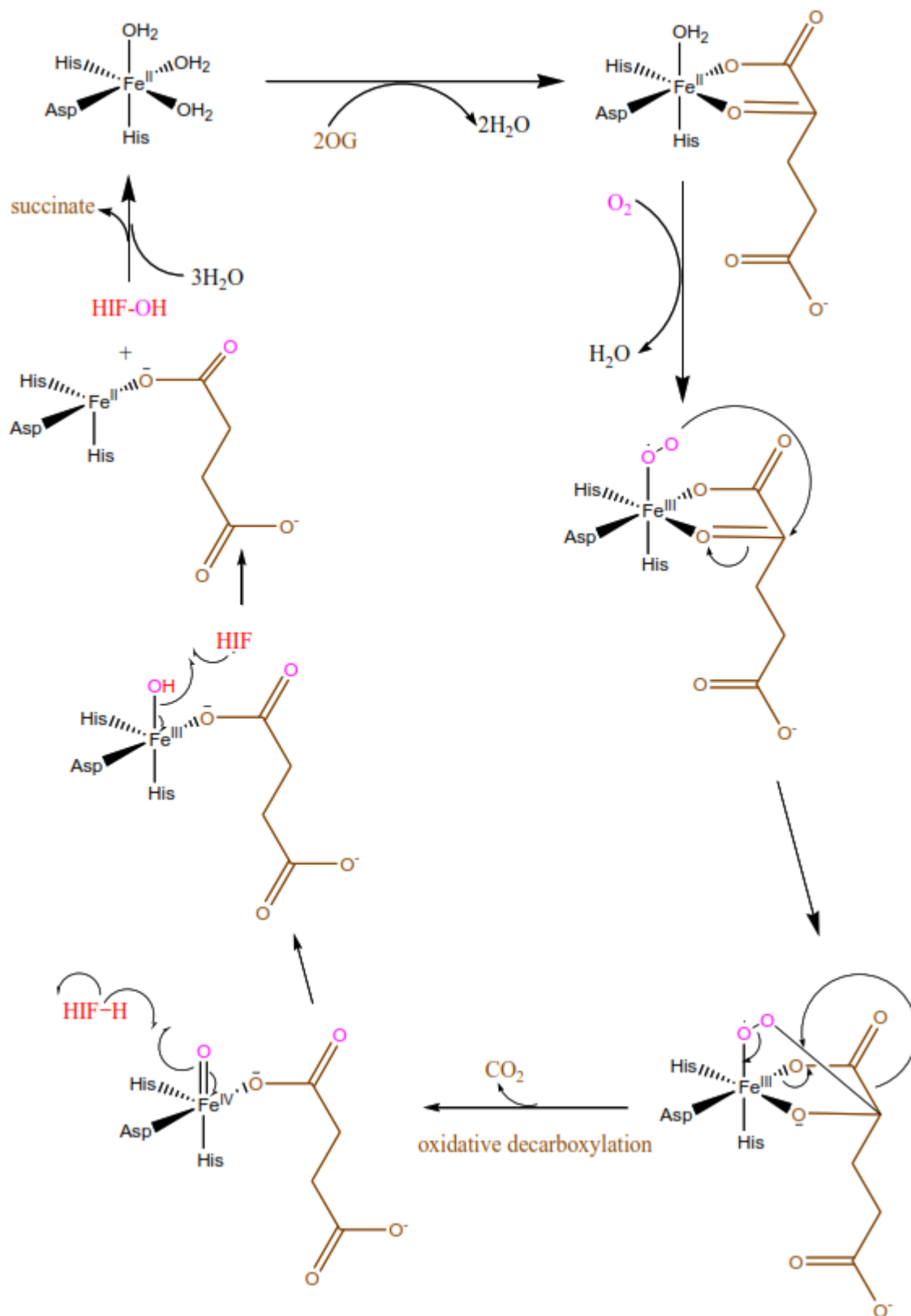
Despite HIF-1 α is ubiquitously expressed, HIF-1 α protein level is regulated by prolyl hydroxylase domain (PHD) enzymes. There are three members in the conserved proline hydroxylase enzyme family known as PHD-1, PHD-2 and PHD-3²⁵. Recently, putative PHD-4 has been reported²⁶. PHD-2 has the highest activity towards the primary hydroxylation site of HIF-1 α and believed to be the main isoform involved in regulating HIF-1 α ^{27,28}.

PHDs belong to an extensive family of 2-oxoglutarate (2OG) dependent, non-haem dioxygenases which utilize oxygen as the co-substrate in hydroxylation²⁹⁻³¹. Hydroxylation is halted during hypoxia due to the low concentration of oxygen present which then restores HIF stability and activity^{29,30}. Therefore, PHDs are regarded as dioxygen sensors.

Beside regulation by PHDs, HIF-1 α is also regulated by Factor inhibiting HIF (FIH). FIH is a member of new sub-family of iron- and 2OG dependent dioxygenases and one of jumonji (JmjC) transcription factors^{32,33}. FIH contains one iron (II) ion coordinated octahedrally by side chains of His199, Asp201 and His279. The HIF hydroxylation reactions are shown in **Scheme 1.1** and the general mechanism of 2OG deoxygenases is shown in **Scheme 1.2**.



Scheme 1.1: The hydroxylation reactions catalyzed by HIF prolyl hydroxylase domains (PHDs) and Factor inhibiting HIF (FIH)³⁰.



Scheme 1.2: The proposed mechanism of action of 2OG dependent oxygenases³⁴.

1.2 HIF signaling pathways

HIF have two different signaling pathways which occur during normoxia and hypoxia. During normoxia, PHDs hydroxylate two critical proline residues (P402 and P564) of HIF-1 α in its oxygen-dependent degradation domains (ODD)³⁵. The proline hydroxylation enables binding of ODD with von Hippel-Lindau tumor suppressor protein (pVHL) to undergo ubiquitination and proteasomal degradation^{12,36,37}. HIF-1 α has a half-life of <5 min and is negatively regulated during normoxia while the constitutive intracellular levels of HIF-1 α is almost undetectable^{2,38-41}.

Besides hydroxylation of proline residues, HIF-1 α is also hydroxylated at the Asn803 residue by Factor inhibiting HIF (FIH)^{35,42,43}. Hydroxylation of Asn803 residue prevents interaction of HIF-1 with p300 and CBP transactivators for transcription of target genes. Both hydroxylation by PHDs and FIH require oxygen, 2-oxoglutarate and iron (II) ion and generates succinic acid and carbon dioxide as byproducts^{13,14,44,45}.

During hypoxia, oxygen concentration is low, activity of PHDs and FIH are reduced. HIF-1 α is then stabilized with reduced binding to pVHL^{12,46}. Next, availability of HIF-1 α to ubiquitination and proteasomal degradation is reduced⁴⁶⁻⁴⁸. Therefore, HIF-1 α hydroxylation activity is reduced and activity of HIF- α subunit is stabilized. HIF-1 α then translocates to the nucleus and dimerizes with HIF-1 β subunit to form heterodimeric activated HIF-1 complex^{39,49,50}. HIF-1 complex then binds to hypoxia responsive elements (HREs) in their target genes to activate various target genes important in adaption to hypoxia such as vascular endothelial growth factor (VEGF) and erythropoietin (EPO)^{1,6,12,22,23,35,41,51-53}. The HIF signaling pathway during normoxia and hypoxia is shown in **Figure 1.2**.

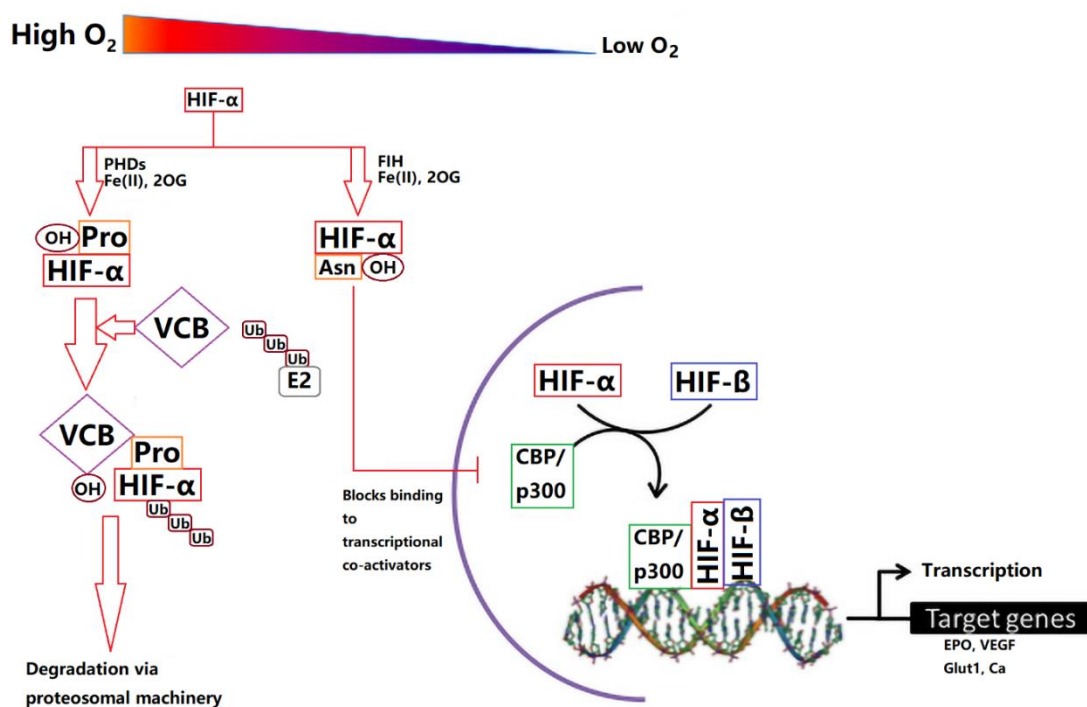


Figure 1.2: HIF signaling pathway during normoxia and hypoxia⁵⁴.

1.3 Problem statement

Inhibition of PHDs have been suggested as an alternative method to upregulate HIF to serve as a treatment to the diseases such as anemia and ischemic diseases⁵⁵. Anemia is considered as a critical disease caused by several factors such as chronic kidney disease (CKD)⁵⁶ and anemia of chronic disease (ACD)⁵⁷. However, the current treatment either cause fluctuation of iron and red blood cells (RBC) or high treatment cost. The discovery of new small molecule inhibitors will make treatment less costly and less dependent on administration of either recombinant erythropoietin or red blood cells. However, current small molecule inhibitors are not effective to replace administration of either recombinant erythropoietin or red blood cells. In this study, different classes of potential PHD-2 inhibitors compounds have been synthesized and tested as potential PHD-2 inhibitors.

1.4 Research objectives

The research objectives:

1. To study the binding affinity of 2H-chromene-3-carboxylic acid, triazine, pyrimidine, benzenesulfonamide and benzoxazolamine as potential PHD-2 inhibitors using computer aided technique (molecular docking)
2. To synthesize and characterize the above mentioned compounds using various spectroscopic methods
3. To study the inhibitory potencies of the synthesized compounds using PHD-2 RapidFire assay
4. To investigate the cell-based studies of the benzoxazolamine analogues to induce HIF-1 α as an indicator of cellular PHD-2 inhibition

1.5 Scopes of study

This study focuses on the synthesis, characterization and inhibitory studies of different classes of compounds (2H-chromene-3-carboxylic acid, triazine, pyrimidine, benzenesulfonamide and benzoxazolamine) against human HIF prolyl hydroxylase domain 2 (PHD-2). The structural design was based on the interactions of these compounds with the PHD-2 enzyme including hydrogen bonding with Arg383 residue and bidentate coordination with the active site iron (II) ion. *In silico* computer aided drug design technique was implemented in the early stages to screen the designed compounds based on Lipinski's Rules, estimation of the free energy of binding and binding pose of the compounds in the active site of PHD-2 enzyme based on the crystallographic structure available from www.pdb.com. Lipinski's Rule of Five states that orally active drug must have less than six hydrogen bond donors, less than eleven hydrogen bond acceptors and below molecular weight of 500 g/mol. Compounds

which showed good binding affinity in molecular docking studies were further synthesized and characterized using various spectroscopic techniques such as nuclear magnetic resonance (NMR) (1D and 2D), mass spectrometry (MS) and Fourier transform infrared spectroscopic (FT-IR). The inhibitory potencies of the compounds were screened using RapidFire PHD-2 hydroxylation assay. The assay was carried out by Dr. Martin Abboud at Chemical Research Laboratory, University of Oxford. The cell-based studies of the benzoxazolamine analogues to induce HIF-1 α as an indicator of cellular PHD-2 inhibition was carried out by Chan Yan Ying at Dr. Andrew Chan Mun Chiang's lab in Department of Molecular Medicine, University of Malaya.

CHAPTER TWO

LITERATURE REVIEW

2.1 HIF target genes

Hypoxia is shown to induce expression of various target genes that encode proteins related to different adaptive responses^{38,50,58-62}. These genes contain essential HIF binding sites required for deoxyribonucleic acid (DNA) transcription activities⁶³⁻⁶⁶. The adaptive responses are induced to deliver oxygen to cells via activation of genes such as transferrin and endothelin-1 and to adapt decreased oxygen concentration through glycolysis via activation of genes such as glucose transporter 1 and lactate dehydrogenase A^{5,35,67,68}.

Examples of genes upregulated during hypoxia are EPO and VEGF. EPO and VEGF play critical roles in adaptive response to systemic and local hypoxia where both are activated during hypoxia⁶⁹. VEGF plays a central role in angiogenesis, vasculogenesis and neovascularization^{70,71}. Examples of transcriptional targets regulated by HIF are shown in **Figure 2.1**.

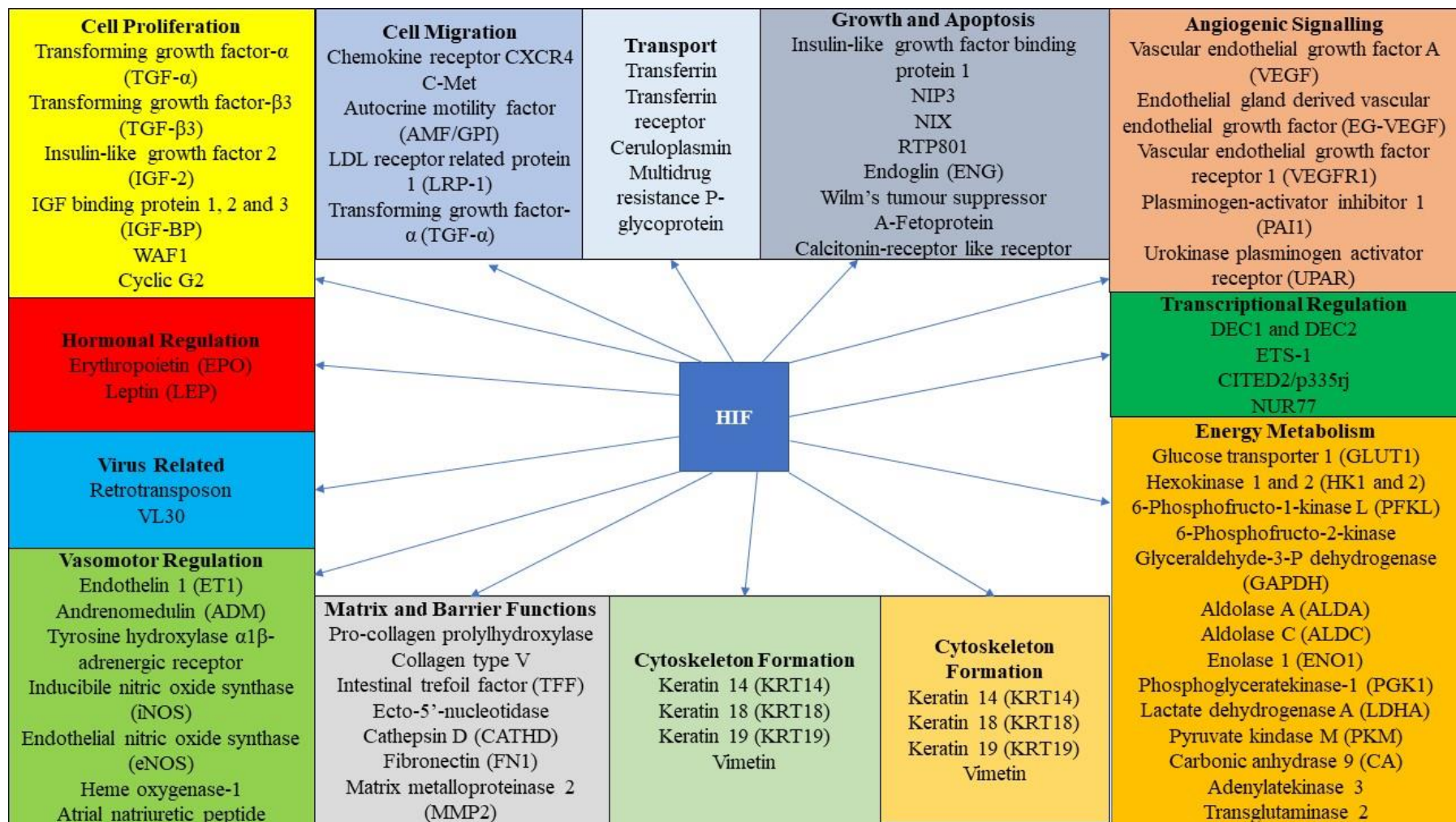


Figure 2.1: The reported transcriptional targets that are regulated by HIF. Adapted from Chowdhury, et al., 2008⁷².

2.2 Therapeutics benefits of HIF activation

PHD inhibition by small molecule inhibitors has been shown to have a significant role in medical treatments. Various treatment strategies which promotes the stability of HIF-1 α protein has been shown to play an important role in cell survival, protection against injury in cell lines and other diseases relating to inflammatory and hypoxic conditions^{66,73-76}. Examples of diseases benefit from the effects of PHD inhibition are ischemia, heart attack, stroke, brain insults, chronic anemia, wounding and inflammation.

In certain cases where surgical intervention is not allowed to remove the disease, PHD inhibition has been reported to be an alternative method to be used^{15,38,62,77-81}. Inhibition of PHD activity by small molecule inhibitors rather than inhibition of PHDs by hypoxia have also been shown to play a role in neuroprotection⁸².

2.3 PHD-2 structural data

Up to date, out of the three PHD enzymes, PHD-2 is the only crystal structure resolved by scientist. **Figure 2.2** shows the crystal structure of 1-chloro bicyclic isoquinoline (BIQ), **1** and iron (II) ion⁸³. The cofactor ferrous ion was buried deeply in the active site pocket, coordinated by three set of amino acid residues (His313, Asp315, His374) in tridentate manner forming the iron (II)/2OG complexes⁸³.

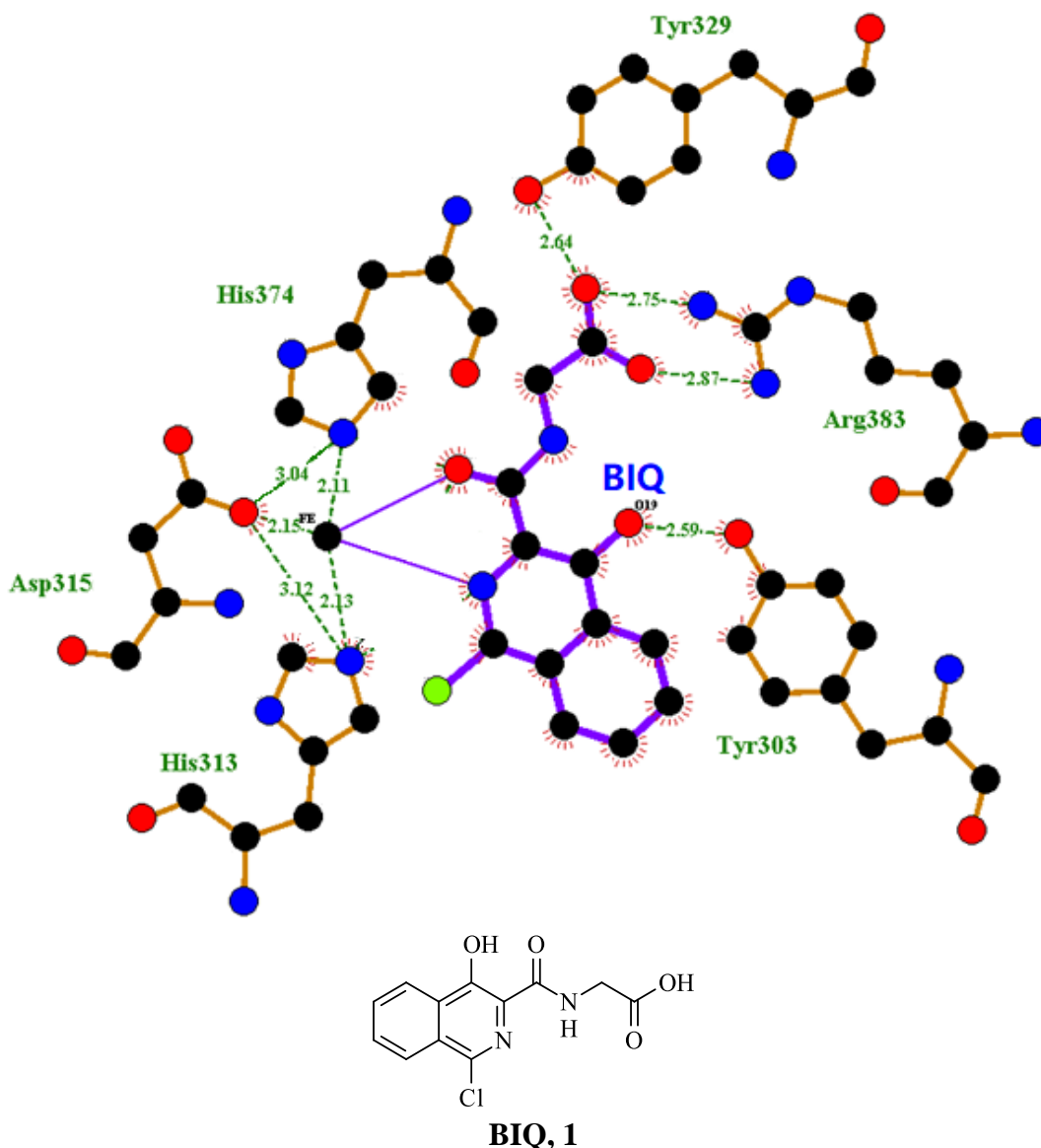


Figure 2.2: Binding interaction of BIQ, 1 with PHD-2 enzyme shown in crystal structure with PDB ID: 2hbt. Data is obtained from Research Collaboratory for Structural Bioinformatics (RCSB) Protein Data Bank (PDB)⁸⁴.

Stabilization of the PHD-2 enzyme with inhibitor bearing aromatic hydrophobic group was due to hydrophobic nature of opening active site with presence of Trp389, Trp258, Met299 and Ile256 residues as shown in **Figure 2.3**⁸⁴. The presence of bulky aromatic ring in PHD-2 inhibitors was an important factor as it helped to prevent HIF-1 α from entering the enzyme binding pocket^{54,86,87}.

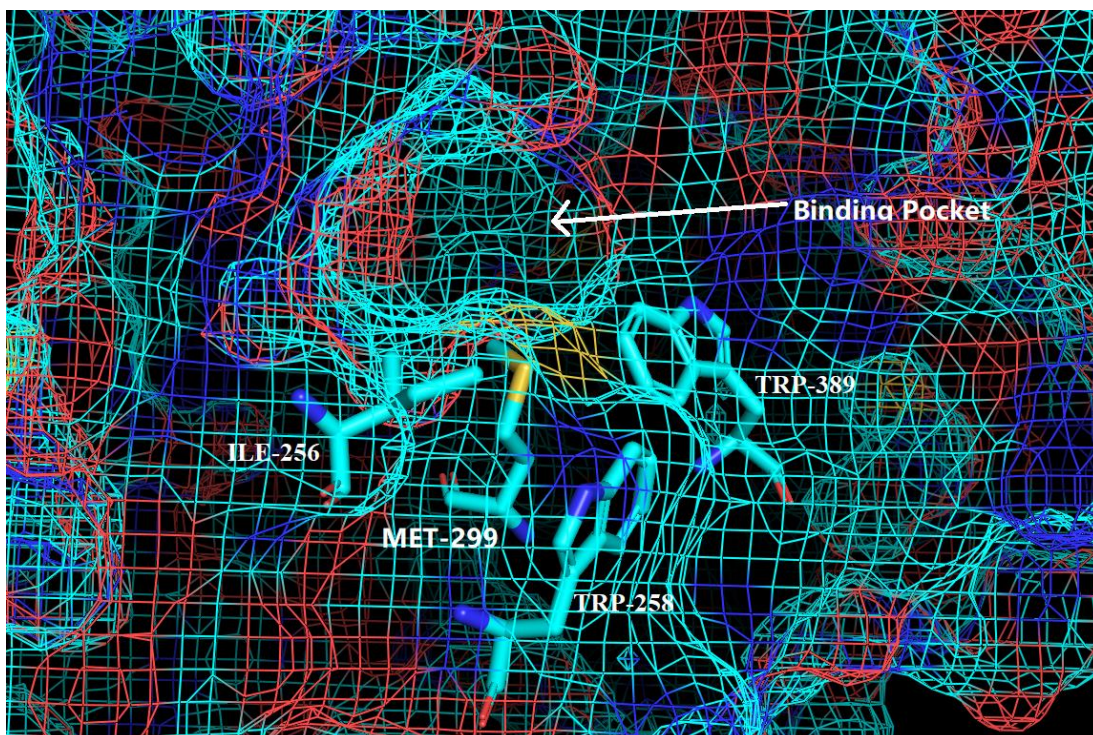


Figure 2.3: PHD-2 binding pocket with presence of Trp389, Trp258, Met299 and Ile256 residues. Data is obtained from RCSB PDB⁸⁴.

2.4 Computer aided drug design (CADD)

Computer aided drug design (CADD) was employed for the inhibitor testing in this study. Since 1960s, docking has become a powerful and essential method in drug screening, protein-ligand interactions and understanding the behavior of nanomaterials. Technologies have dominated the current field of CADD in structural-based drug design to dock ligands into receptors or proteins with many commercial drugs designed from this method¹¹⁵⁻¹¹⁷.

Computational methods are preferred to be used to select potential ligands for experimental testing due to high cost and time consuming for traditional high-throughput screens. CADD method can be used to estimate the binding affinity and binding mode of ligand to the drug target in short period of time. CADD has important role in therapeutic applications due to the improvement of structural studies on

biological molecules which helps in computational approaches for small molecule docking and virtual screening of candidate compounds. Potent and selective inhibitors are designed by medicinal chemists utilizing three-dimensional structures of various protein targets¹¹⁵⁻¹¹⁷.

Structural information of binding site obtained from X-ray crystal structures are used in protein-ligand docking methods¹¹⁸. The increase in numbers of high-resolution crystal structure of receptors in recent years bring to an increase in computation studies of molecular docking. Potential ligands can be identified once structural information about macromolecular drug target is known. There is a growing interested in pharmaceutical industry due to increase in accuracy. Binding affinities of selected ligands are predicted via associating scoring functions with potent ligand chosen from the best binding affinity to run further biochemistry experiments and development¹¹⁹⁻¹²¹.

Drug or inhibitor design process determines the binding and orientation of a ligand in a protein receptor complex which utilizes computational technologies. Computational technologies enable rapid identification of hit and lead compounds. Binding mode and affinity are important in designing therapeutic interventions. Binding mode is the pose with lowest energy score predicted as the best match. Binding affinity is the strength of the binding interaction between ligands and receptor^{119,121}. Knowledge of biological target of interest is used to optimize the process of finding new modifications.

Identification of biological target of interest is the early step in virtual screening¹²². Virtual screening utilizes docking as routine in drug screening and design and performs docking for large number of compounds to determine the putative leads with

given modelled structure of receptor^{120,123,124}. Compounds search via this method is pharmaceutically interesting at a higher rate with a lower cost.

There are two types of virtual screening: ligand-based virtual screening and structure-based virtual screening. Properties of set of ligands known to bind to the receptor in interest are important for a ligand's biological effects in ligand-based virtual screening. For structure-based virtual screening, ligands are the physical entities and scoring function is used to predict the binding site of interest.

After structures of ligands and proteins are prepared, energy minimization is utilized to determine the most stable 3D confirmation. Ligands are drawn and protein to be docked can be downloaded from PDB with focus on higher X-ray resolution for better accuracy.

2.4.1 Docking and root mean square deviation (RMSD)

Docking is a very important technique for understanding interaction of chemical compounds with enzymes. It is also a simple technique because it requires very low equipment to run. Docking begins with the idea of 'lock and key' drug design. Protein-ligand docking usually involves sampling algorithms and scoring functions. Sampling algorithms in docking software is used to explore the possible binding modes of ligand in the protein-ligand complex while scoring function is used to estimate relative binding affinities and rank ligand poses^{121,125-127}.

Docking focuses on creating the correct conformation of the designed compound in the receptor with the cocrystalline compound. Root mean square deviation (RMSD) value refers to the ability of the docking programs to replicate the binding mode of

reported compound with the cocrystalline compound in the target protein. Values threshold of RMSD below 2 Å between reported and cocrystalline compounds are statistically the most frequently used to predict the success rate while RMSD below 1.5 Å was preferred for smaller compounds^{128–132}. In this study, PyMOL 2.0.7 by Schrödinger, LLC was used to determine the RMSD of the designed compounds.

2.5 PHD inhibitors

The hydroxylation of HIF by PHDs requires oxygen, 2OG and iron (II) ion. There are a few classes of PHDs reported inhibitors, including iron chelators, transition metal ions and mimetic 2OG inhibitors. The carboxylate group in mimetic 2OG inhibitors was shown to compete with 2OG in the enzyme binding pocket in certain studies⁵⁴. The design of carboxylate appendage inhibitors was focused in study.

2.5.1 Iron chelators

Iron chelators inhibit PHDs by chelating the iron (II) ion active site, hence, the enzymes lose its function to hydroxylate HIF. Three reported PHD inhibitors which work via chelation of iron are desferrioxamine (DFO), **2**, clioquinol, **3** and ciclopirox, **4**. Their structures are shown in **Figure 2.4**. These iron chelators are able to upregulate HIF-1 α levels, but failed to upregulate erythropoietin plasma^{38,40,88}. Clioquinol and ciclopirox are low-affinity inhibitors which are not selective for PHD-2 enzyme⁸⁸.

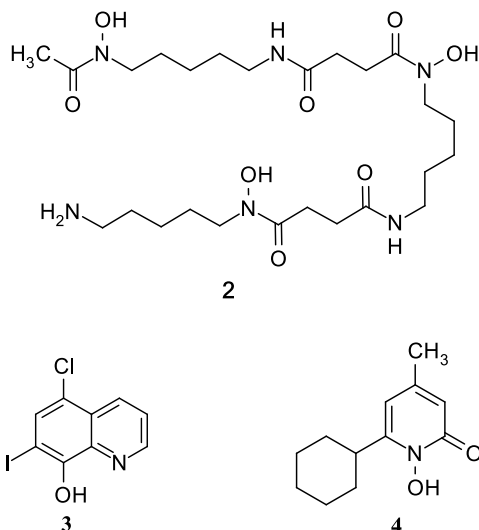


Figure 2.4: Structures of different iron chelators: **2**, **3** and **4**.

2.5.2 Transition metal ions

Transition metal ions inhibit PHDs by displacing the iron (II) ion active site. Examples of transition metal ions inhibitors are Co^{2+} , Ni^{2+} , Zn^{2+} , Cu^{2+} , Cd^{2+} and Mn^{2+} ^{89,90}. The half-maximal inhibitory concentration (IC_{50}) against PHD-2 by transition metal ions are summarized in **Table 2.1**.

Table 2.1: Reported IC_{50} values of the transition metal ions against PHD-2⁹⁰.

Metal ions	Co^{2+}	Ni^{2+}	Zn^{2+}	Cu^{2+}	Cd^{2+}	Mn^{2+}
IC_{50} (μM)	48.3	185.2	9.3	6.6	57.4	21.0

2.5.3 2-Oxoglutarate (2OG) mimetic inhibitors

2OG mimetic inhibitors are compounds that have similar structures as 2OG, **5**. They can compete with co-substrate 2OG to chelate the metal ion and form hydrogen bonding in the active site of PHD-2. Examples of 2OG mimetic inhibitors are N-oxalylglycine (NOG)⁹¹, thiazol analogues⁹², pyrazole analogues^{34,93-95}, pyridine

analogues^{34,93,96,97}, pyrimidine⁹⁸, benzodiazole analogues^{94,99} and bicyclic isoquinoline analogues^{97,100–102}.

2OG mimetic inhibitors have similar binding interaction in the PHD-2 active site as the co-substrate 2OG. The crystal structure of **2OG** in PHD-2 is shown in **Figure 2.5**. Bidentate coordination with the iron (II) ion active site are formed from the oxygen atoms while salt bridge with Arg383 residue and hydrogen bonding with Tyr329 residue are formed from oxygen atoms in the carboxylate group⁹⁴.

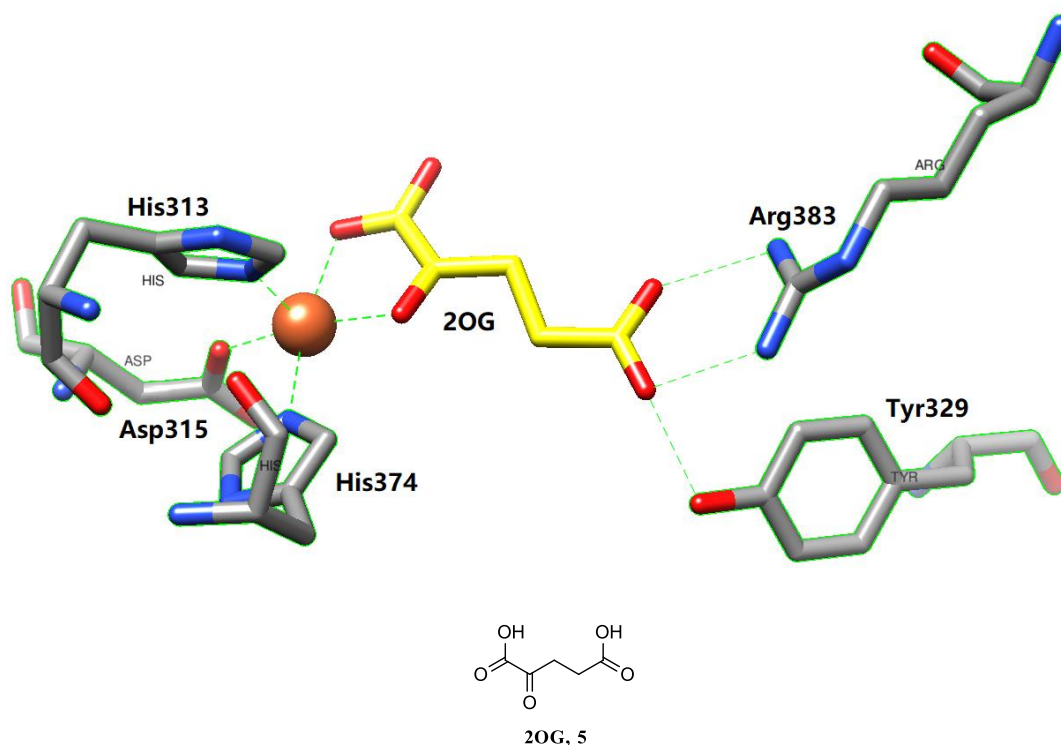


Figure 2.5: The crystal structure of PHD-2 active site with **2OG**. **2OG** is shown in yellow while iron (II) is shown in brown⁹⁴. Data is obtained from RCSB PDB⁸⁴.

2.5.3(a) N-oxalylglycine (NOG) and dimethyl N-oxalyl-glycine (DMOG)

NOG, **6** has been shown to inhibit PHDs in competition with **2OG**. An ester derivative form of **NOG**, DMOG, **7** is a cell permeable prodrug of **NOG** which penetrates the cells to form **NOG**. The process is reported to be catalyzed by cellular

carboxylesterases^{13,103}. **DMOG** is shown to inhibit activity of both PHDs and FIH and upregulate HIF-1 and HIF activity in animals^{80,104}. IC₅₀ value of **NOG** against PHD-2 is shown in **Figure 2.7**. The binding interaction of **NOG** is shown in **Figure 2.6**.

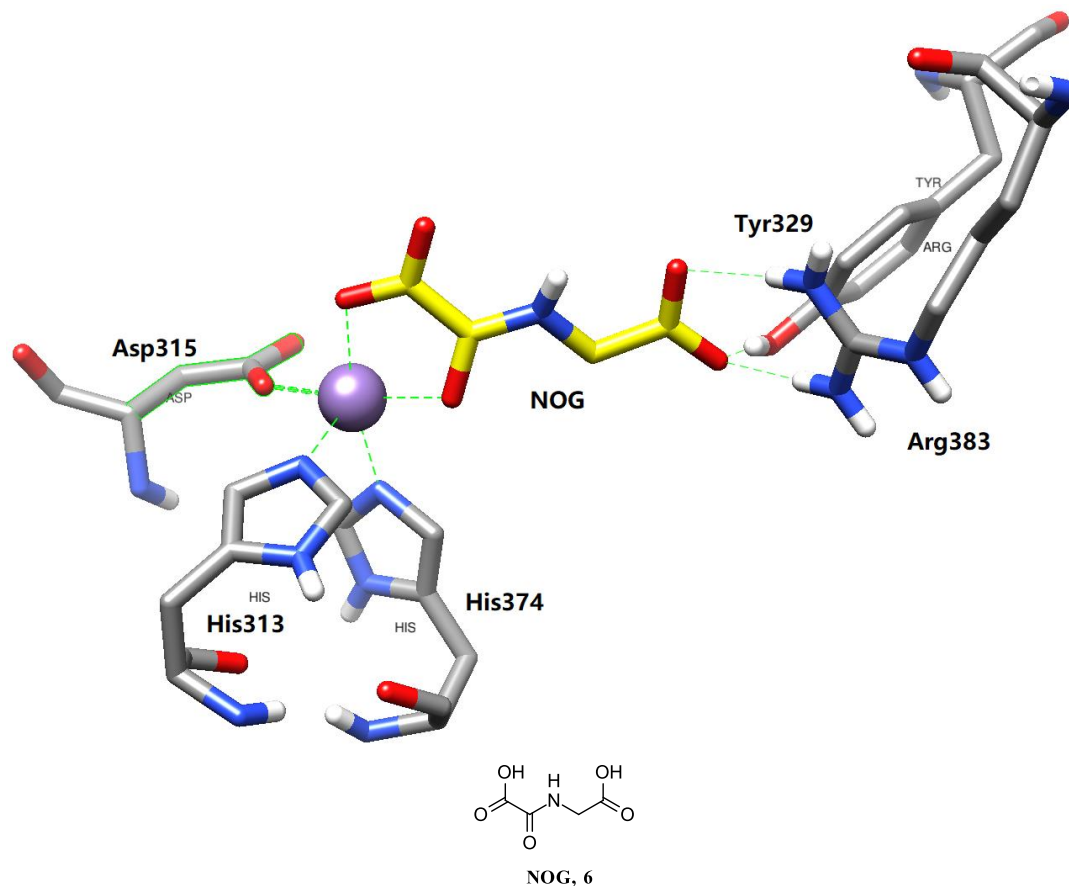


Figure 2.6: The crystal structure of PHD-2 active site with **NOG, 6**. **NOG, 6** was shown in yellow while manganese (II) was shown in purple was used instead of iron (II)⁹¹. Data is obtained from RCSB PDB⁸⁴.



Figure 2.7: **NOG, 6** and **DMOG, 7** with reported IC₅₀ values of **NOG** (6.2¹⁰⁵ μM) against PHD-2.

2.5.3(b) Thiazol and pyrazole analogues

A series of thiazol and pyrazole analogues were reported as PHD-2 inhibitors. The thiazol compound **8** with a benzene ring further away from the thiazol group and carboxylate side chain closer to the thiazol group was shown to have better inhibition potency compared to compound **9**. On the other hand, the pyrazol compounds **12** and **14** with a bicyclic ring structure seems to exhibit better inhibition potency compared to compounds (**11**, **13** and **15**) with monocyclic ring structure. The position of the benzene ring of compounds (**8**, **9** and **10**) further away from the thiazol group might exhibit better inhibition potency due to better fitting in the narrow active site of PHD-2 enzyme. Bicyclic ring structures (**12**, **14** and **16**) showed to have better inhibition value in pyrazole analogues might be due to the resonance of the electrons in the ring structure which favors the coordination bond with the iron (II) ion. The structures of thiazol (**8 - 10**) and pyrazole analogues (**11 - 16**) were shown in **Figure 2.8** and their IC_{50} values against PHD-2 were summarized in **Table 2.2**. An example of crystal structure of pyrazol compound **16** in PHD-2 active site is shown in **Figure 2.9**. Bidentate coordination with the active site iron (II) ion are formed from the nitrogen atom in benzimidazole and pyrazole while salt bridge with Arg383 residue and hydrogen bonding with Tyr329 residue are formed from oxygen atom in carboxylate group.

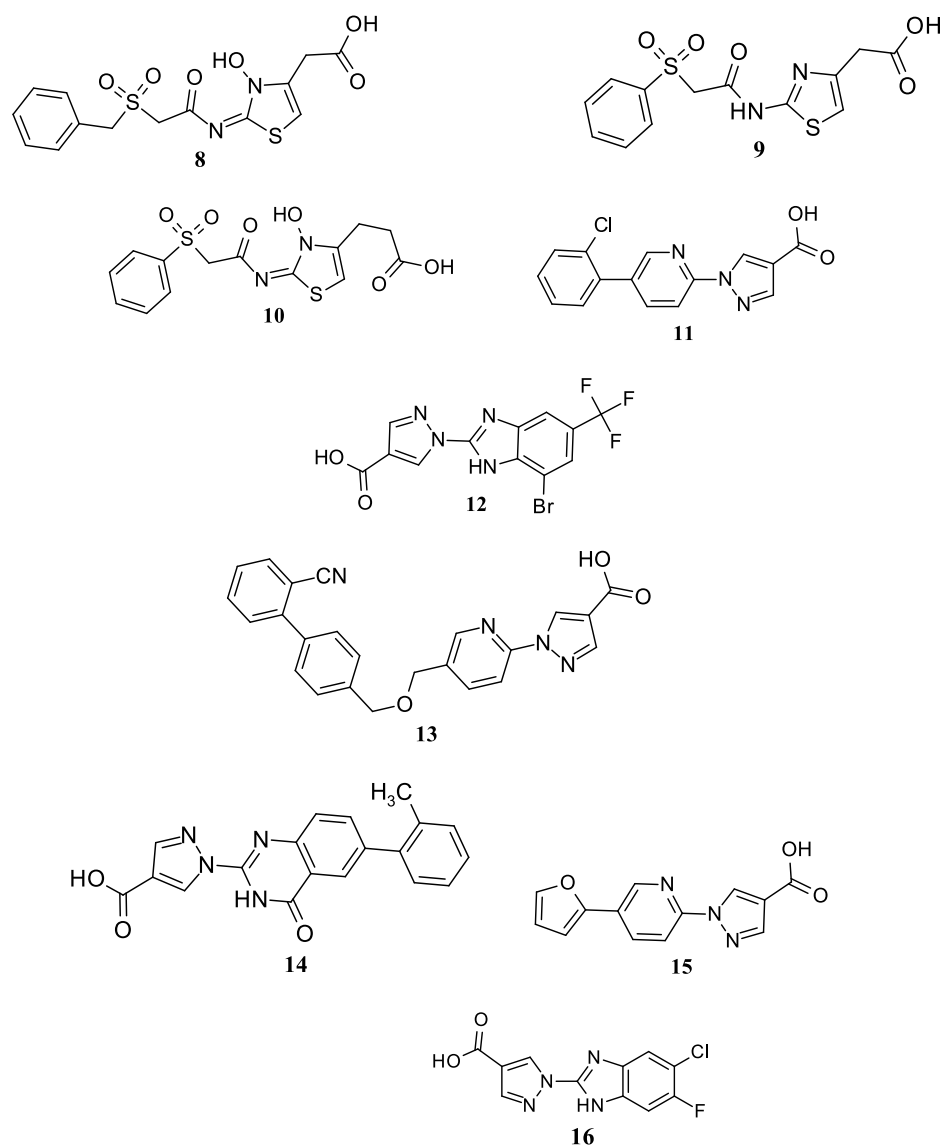


Figure 2.8: Thiazol analogues (8 – 10) and pyrazole analogues (11 – 16).

Table 2.2: Reported IC_{50} values of thiazol analogues (8 – 10) and pyrazole analogues (11 – 16) against PHD-2.

Compound	8	9	10	11	12	13	14	15	16
IC_{50} (μM)	0.011 ⁹²	40 ⁹²	0.41 ⁹²	6.5 ⁹³	0.1585 ⁹⁴	0.19 ⁹⁵	0.008 ³⁴	15 ⁹³	0.07943 ⁹⁴

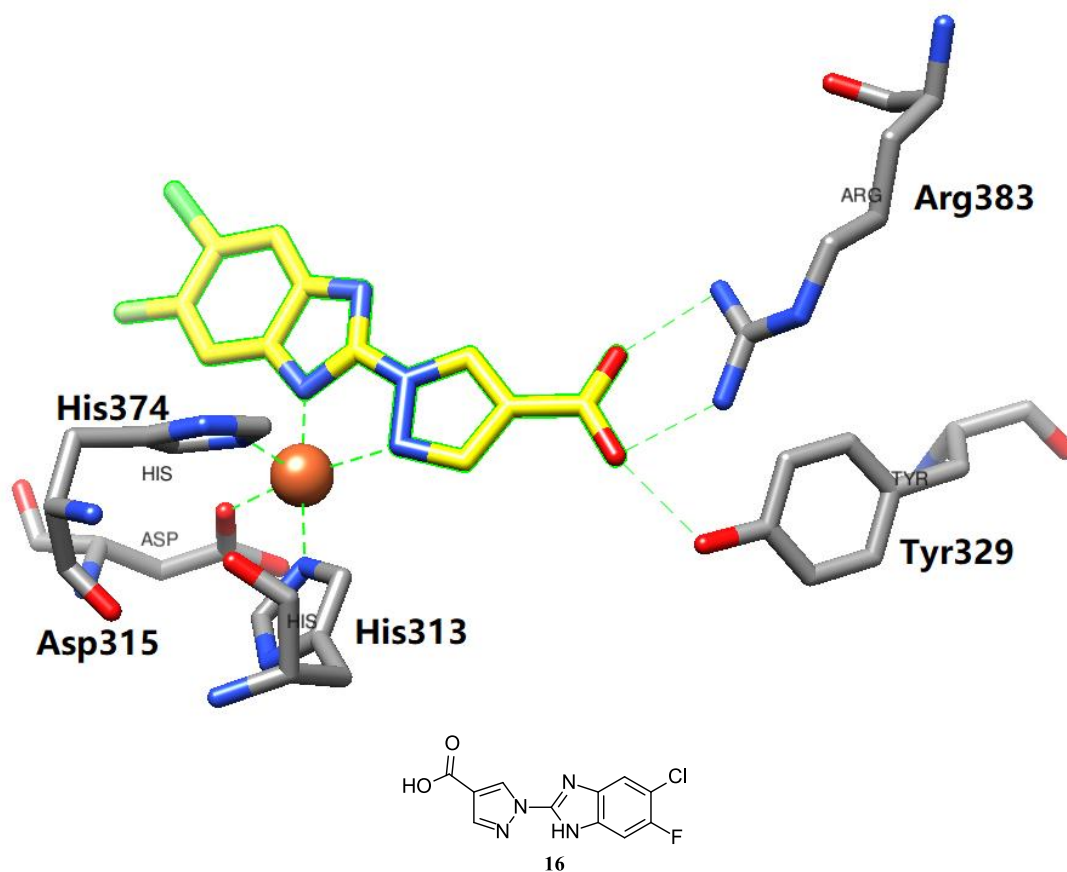


Figure 2.9: The crystal structure of PHD-2 active site with 1-(5-chloro-6-fluoro-1H-benzimidazol-2-yl)-1H-pyrazole-4-carboxylic acid, **16**. **16** was shown in yellow while iron (II) was shown in brown⁹⁴. Data is obtained from RCSB PDB⁸⁴.

2.5.3(c) Pyridine analogues, pyridinol analogues and pyrimidine

A series of reported pyridine analogues, pyridinol analogues and pyrimidine potent PHD-2 inhibitors are shown in **Figure 2.10**. Compound **18** with additional monocyclic ring away from the carboxylic group with the purpose of blocking the entrance of the PHD-2 active site does not give better inhibition value compared to compound **17** which does not have any benzene ring structure that blocks the entrance of the PHD-2 active site. This might be due to the absence of the hydroxyl group in the aromatic ring because compounds **19** – **23** have hydroxyl group in the aromatic ring adjacent to the carboxylic group. The crystal structure of compounds **22** and **23** were shown in **Figure**

2.11 and **Figure 2.12**, respectively. The IC_{50} values of pyridine analogues, pyridinol analogues and pyrimidine were shown in **Table 2.3**.

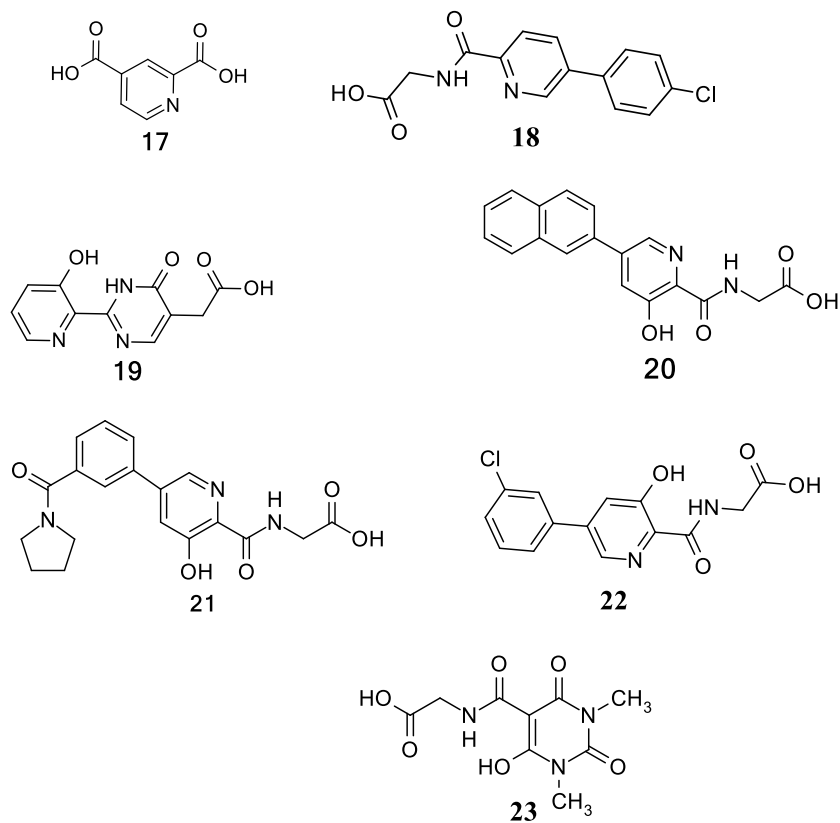


Figure 2.10: Pyridine analogues (**17 - 18**), pyridinol analogues (**19 - 22**) and pyrimidine (**23**).

Table 2.3: Reported IC_{50} values of pyridine analogues (**17 - 18**), pyridinol analogues (**19 - 22**) and pyrimidine (**23**) against PHD-2.

Compound	17	18	19	20	21	22	23
IC_{50} (μ M)	2^{97}	15^{93}	27.5^{106}	0.017^{34}	0.3^{107}	0.029^{98}	0.067^{98}

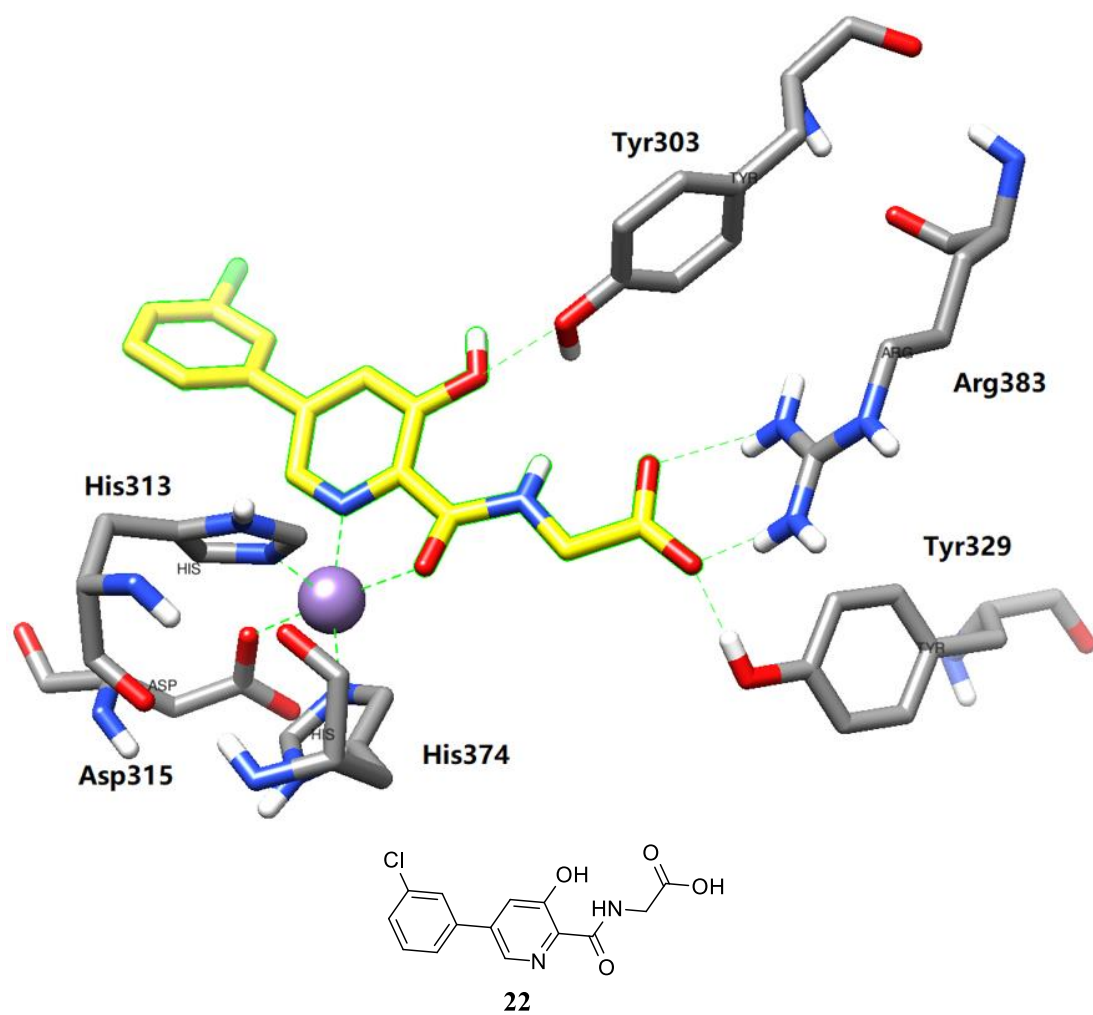


Figure 2.11: The crystal structure of PHD-2 active site with Vadadustat, **22**. **22** was shown in yellow while manganese (II) (substituting iron (II)) was shown in purple⁹⁸. Data is obtained from RCSB PDB⁸⁴.

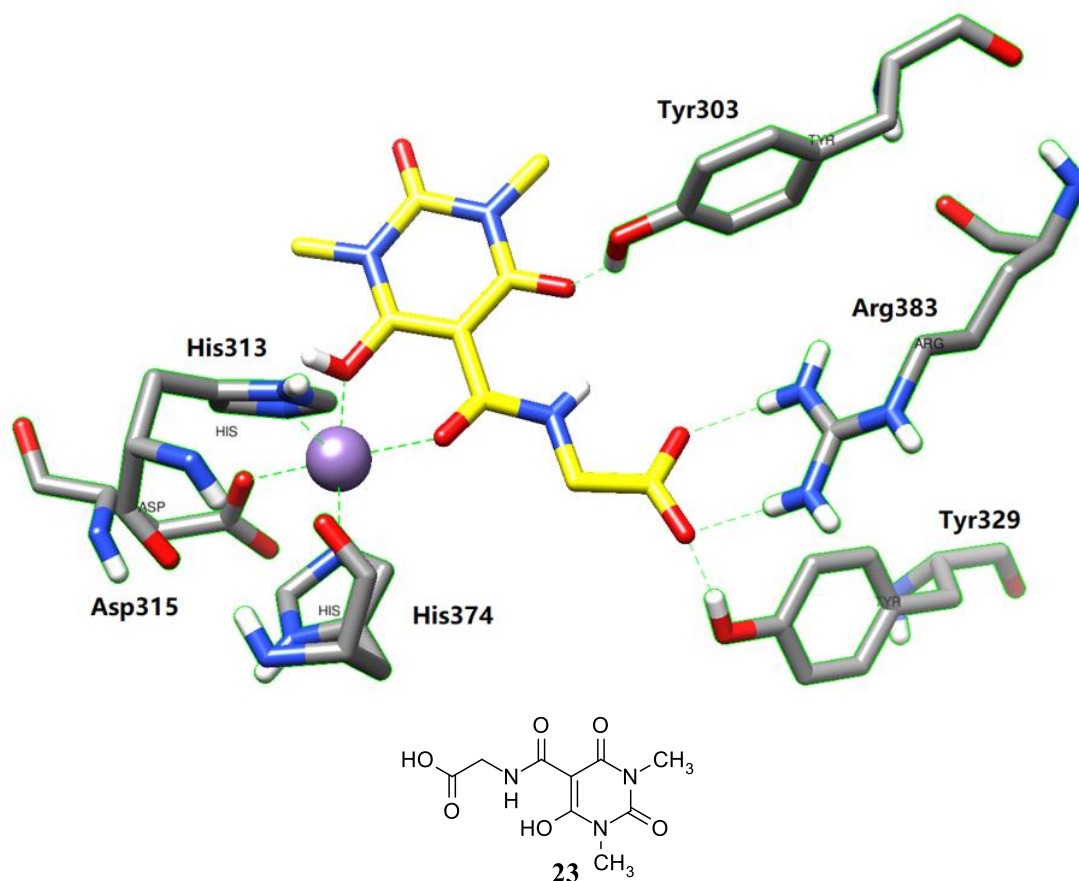


Figure 2.12: The crystal structure of PHD-2 active site with (6-hydroxy-1,3-dimethyl-2,4-dioxo-1,2,3,4-tetrahydropyrimidine-5-carbonyl)glycine, **23**. **23** was shown in yellow while Mn(II) (substituting Fe(II)) was shown in purple⁹⁸. Data is obtained from RCSB PDB⁸⁴.

2.5.3(d) Benzodiazole analogues

Examples of benzodiazole analogues that were reported as potent PHD-2 inhibitors were shown in **Figure 2.13**. The inhibition potency is higher when there is a benzene ring attached to the bicyclic ring structure as shown in compound **25**. The crystal structure of benzodiazole analogues were shown in **Figure 2.14** and the IC₅₀ values were shown in **Figure 2.13**. Bidentate coordination with the iron (II) ion active site are formed from the oxygen atom in amide group and nitrogen atom in benzimidazole group while salt bridge with Arg383 residue and hydrogen bonding with Tyr329 residue are formed from oxygen atom in carboxylate group as shown in **Figure 2.14**⁹⁴.